IET Microwaves, Antennas & Propagation

Research Article

IET Journals
The Institution of Engineering and Technology

Sector nulling in planar irregular sub-arrayed sparse array antennas

ISSN 1751-8725
Received on 24th October 2014
Revised on 8th July 2015
Accepted on 9th July 2015
doi: 10.1049/iet-map.2014.0712
www.ietdl.org

Asim Ali Khan[1] ✉, *Anthony Keith Brown*[2]

[1]*Electrical Engineering Department, COMSATS Institute of Information Technology, Lahore, Pakistan*
[2]*School of Electrical and Electronic Engineering, University of Manchester, Manchester, England*
✉ *E-mail: asim.khan@theiet.org*

Abstract: This study concerns wide angular sector (higher order) null synthesis in planar irregular sparse antenna arrays when aperture distributed sub-arrays are used to reduce the computational load. A hybrid optimisation tool has been used to find array element excitations to achieve as low as possible sector nulls for the desired sector width. Performance comparisons have been made for three sub-array configurations based on the obtained numerical results. Various interference jamming scenarios have been considered including single and dual sectors for single-dimensional (θ) (1D) and two-dimensional (θ, ϕ) (2D) nulls. The proposed optimisation scheme has shown to be successful for the synthesis of 1D and 2D sector nulls with depths as low as −100 dB for the given configuration with reduced computational time when compared with the full array. The comparison of achieved null depths for different sub-array sizes and convergence time has also been presented and discussed.

1 Introduction

Sparse arrays offer wideband, low cost and potentially light weight solution for various applications, for example, airborne, space-borne platforms and radio astronomy. Under circumstances when it is not possible to identify the exact location of a noise source or when the noise source is broadband, it is necessary to have an array with broad angular sector nulling capability if null steering techniques are used to improve the system signal-to-noise ratio. Various methodologies including sub-arrays and adaptive nulling have reported in the literature for wide sector nulling in regular antenna arrays [1–16]. Although in principle for uniform linear arrays $N-1$ nulls are steerable, in practice steering these nulls to cancel interference can cause serious overall pattern degradation (e.g. higher sidelobe levels). A simple criterion which can be found in literature for uniformly spaced arrays to produce nulls in a desired direction is that the total number of interferers should be less than or equal to half of the total number of nulls [2]. If this criterion is satisfied, reasonable sidelobe level control may be achieved in addition to the prescribed nulling.

Unfortunately, determination of the total number of independent nulls is not straight forward in case of irregular sparse antenna arrays. To the best of authors' knowledge, very little or no attention is given to sector nulling in irregular sparse planar antenna arrays. However, [17] addresses the problem of applying the precision nulls in planar sparse antenna arrays. The reported work covers the narrowband nulling in multiple directions but the wide sector and wideband nulling have not been addressed.

This paper considers sector nulling in irregular sparse antenna arrays and investigates the effect of sub-arrays on convergence and nulling performance in terms of sector width and null depth. It has shown that for any given geometry, the use of sub-arrays is beneficial in large irregular sparse antenna arrays due to the ability to optimise sub-array solutions in parallel. Single dimension sector nulling performance (in both null width and depth) has compared for the sub-array size and convergence time. Sub-arrays with smaller numbers of elements converge faster but show compromised nulling performance in terms of average null depths. A hybrid optimisation scheme consisting of a particle swarm optimiser and a sequential quadratic programing (Hy-PSO-SQP) [17] has used to meet the design objectives by tuning the complex array excitations. The proposed method may be applied to achieve two-dimensional (2D) nulls as demonstrated in this communication. The optimisation objectives are set such that the array gain in the bore-sight direction has maximised with sector null depths as low as possible. It has been shown that the proposed sub-arraying technique may also be used to achieve dual sector nulls.

2 Formulation and technique

For any arbitrary planar array consisting of N elements, the array factor is given by the following equation

$$\mathrm{AF}(u, v) = \sum_{n=1}^{N} a_n e^{\mathrm{j}[x(n)ku + y(n)kv]} \tag{1}$$

where 'k' is the wavenumber, $u(\theta, \phi) = \sin\theta\cos\phi$, $v(\theta, \phi) = \sin\theta\sin\phi$, $x(n)$ and $y(n)$ define the position of nth element in x–y plane. The element positions are determined randomly for given aperture size '$X \times Y$', N and minimum allowed separation 'd'. For this work, no pattern features (e.g. sidelobe levels, beamwidths etc.) were constrained at this stage and any arbitrary array geometry fulfilling $d \geq 1\lambda$ may be selected [17].

A pseudorandom process has used for the element selection in 'M' sub-arrays of 'P' elements [17] and each sub-array is solved separately, ideally in parallel. It is important to consider that sub-array elements are distributed across the whole aperture as this ensures that all such sub-arrays would have approximately the same half-power beamwidth (HPBW). This requirement limits the number of possible sub-arrays for any given application as there will be less number of elements in a single sub-array. These elements will spread across the entire array aperture and will have extensive inter-element separation that will cause more grating lobes. These grating lobes will challenge the radiation pattern synthesis procedure using element excitations due to fewer elements per sub-array.

This condition is required to be fulfilled for successful implementation of superposition principle.

Sub-array factor for mth sub-array of P elements is given by the following equation

$$\mathrm{SAF}_m(u, v) = \sum_{p=1}^{P} a_p \mathrm{e}^{\mathrm{j}[x_m(p)ku + y_m(p)kv]} \tag{2}$$

where $x_m \in x$ and $y_m \in y$ are coordinates for elements in mth sub-array. Full-array factor that sums up M sub-arrays by superposition principle is given by the following equation

$$\mathrm{FAF}(u, v) = \sum_{m=1}^{M} \sum_{p=1}^{P} a_{mp} \mathrm{e}^{\mathrm{j}[x_m(p)ku + y_m(p)kv]} \tag{3}$$

where a_{mp} is the excitation coefficient of pth element in mth sub-array.

Since the optimisation problem considered for this work is a multi-objective problem as the array maxima is desired in the broadside direction and reduced radiation level is desired in target angular sector. This is modelled as a single objective problem by implementing a weighted sum approach. The fitness function to be minimised is given by the following equation

$$\Psi = \zeta_1 \frac{1}{|\delta|} + \zeta_2 \frac{1}{D_\mathrm{a}} \tag{4}$$

where Ψ is the value of the fitness function at any given iteration, ζ_1 and ζ_2 are weighting coefficients, δ is the maximum radiation level across the angular sector $\Delta\theta_\mathrm{c}$ centred at θ_c, given by (5) and D_a is the array directivity. In case of single sector nulling

$$\delta = \max\left(\mathrm{SAF}_m^\mathrm{n}\left(u(\Delta\theta_\mathrm{c},\ \phi_g\right), v(\Delta\theta_\mathrm{c}, \phi_g)\right) \tag{5a}$$

$$\delta = \max\left(\mathrm{AF}_\mathrm{n}\left(u(\Delta\theta_\mathrm{c},\ \phi_g\right), v(\Delta\theta_\mathrm{c}, \phi_g)\right) \tag{5b}$$

where $\mathrm{SAF}_m^\mathrm{n}$ is the normalised sub-array factor and AF_n is the normalised array factor. Equation (5a) is used for mth sub-array and (5b) for full-array optimisation scenario.

This method is also applied to obtain dual sectors and (5) is modified as

$$\delta = \max\begin{pmatrix} \mathrm{SAF}_m^\mathrm{n}\left(\left(u(\Delta\theta_\mathrm{c}',\ \phi_g\right), v\left(\Delta\theta_\mathrm{c}', \phi_g\right)\right), \\ \mathrm{SAF}_m^\mathrm{n}\left(\left(u(\Delta\theta_\mathrm{c}'',\ \phi_g\right), v\left(\Delta\theta_\mathrm{c}'', \phi_g\right)\right) \end{pmatrix}. \tag{6}$$

where $\Delta\theta_\mathrm{c}'$ and $\Delta\theta_\mathrm{c}''$ are the target null sectors centred across two different θ_c' and θ_c''.

In case of 2D nulls, the radiation pattern is desired to be reduced over a patch in $u - v$ space. For simplicity, this can be achieved by defining the 2D sector as $(\Delta\theta_\mathrm{c},\ \Delta\phi_\mathrm{c})$ centred at $(\theta_\mathrm{c},\ \phi_\mathrm{c})$. The fitness function modifier δ in (4) will have a new form to achieve 2D nulls

$$\delta = \max\left(\mathrm{SAF}_m^\mathrm{n}\left(u(\Delta\theta_\mathrm{c},\ \Delta\phi_\mathrm{c}\right), v(\Delta\theta_\mathrm{c},\ \Delta\phi_\mathrm{c})\right) \tag{7}$$

To achieve dual 2D sectors, (6) is modified as follows

$$\delta = \max\begin{pmatrix} \mathrm{SAF}_m^\mathrm{n}\left(\left(u(\Delta\theta_\mathrm{c}',\ \Delta\phi_g'\right), v\left(\Delta\theta_\mathrm{c}', \Delta\phi_g'\right)\right), \\ \mathrm{SAF}_m^\mathrm{n}\left(\left(u(\Delta\theta_\mathrm{c}'',\ \Delta\phi_g''\right), v\left(\Delta\theta_\mathrm{c}'', \Delta\phi_g''\right)\right) \end{pmatrix}. \tag{8}$$

2.1 Hybrid particle swarm optimiser and sequential quadratic programming

Heuristic techniques are suitable for the non-linear optimisation problems such as the optimisation of non-uniformly spaced arrays. However, these techniques suffer by the exponential rise of computational time with the increase of number of variables. Therefore, for non-linear problems with large variable space, heuristic methods are paired with the non-linear deterministic methods for their ability to converge faster to find optimum solutions with overall faster convergence rate [17]. To find out the starting point for the initiation of deterministic solution, heuristic optimiser is required to run for less number of iterations to find the appropriate starting point. Once a point is determined, it is used to find the solution by applying the deterministic approach.

The optimisation tool used in this work is hybrid of PSO [18] and SQP [19]. Details on the hybrid technique and its comparison with other schemes have reported in [17]. The optimisation process has been divided into two steps: first step involves PSO in order to define an initial or starting point for the SQP algorithm; in second step, SQP is initiated with the outcome from PSO. For this purpose, PSO is run for 30 iterations and complex weights obtained are used to initiate SQP. This hybrid operation enables faster convergence and may be useful for large antenna array optimisations.

3 Numerical results

A sparse array of elements arranged in a circular outline has assumed for this study with $N = 120$ as shown in Fig. 1. The diameter was 15λ and element positions were determined by applying the pseudorandom process given in [17]. For the geometry selection, no constraints are applied to the radiation pattern features and elements are allowed to appear anywhere with equal likelihood. While the minimum allowed element separation is set to 1λ and the average separation is found to be $1.08\ \lambda$.

For this study, three sub-array configurations have been considered and the average separation in each sub-array is listed in Table 1. Configuration 1 (Config. #1) consists of two sub-arrays, 60 elements each, as shown in Fig. 2*a*, with average element separation 1.25λ. Configuration 2 (Config. #2) has four sub-arrays, 30 elements each and average element separation of 1.48λ, as shown in Fig. 2*b*. Configuration 3 (Config. #3) has eight sub-arrays, 15 elements each and average element separation of 1.95λ, as shown in Fig. 2*c*.

Fig. 3 compares the performance of sector null synthesis when the proposed optimisation scheme has applied to sub-array and full-array configurations. The imposed sector width is 10^o in the region $40^\mathrm{o} \leq \theta \leq 50^\mathrm{o}$ in $\phi = 30^\mathrm{o}$ plane. For all configurations, optimisation objectives were set to achieve null depths as low as possible and

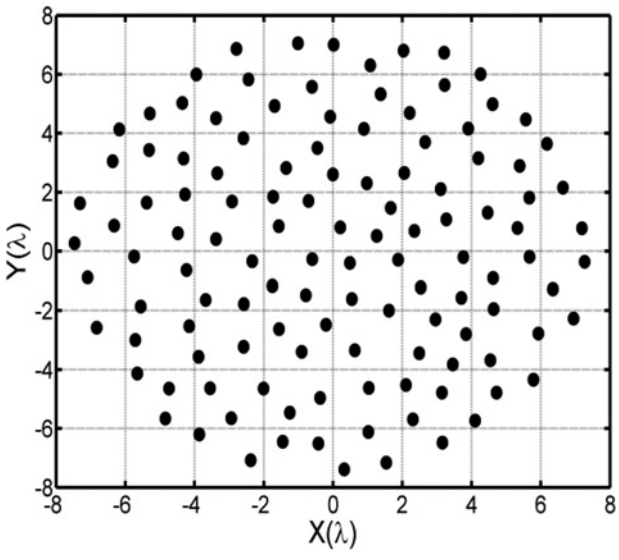

Fig. 1 *Irregularly spaced elements in sparse array geometry $N = 120$, termed as full array*

Table 1 Average element separations in wavelengths (λ) for sub-array configurations used

Array configuration	Average element separation, λ
full array	1.08
Config. #1	1.25
Config. #2	1.48
Config. #3	1.95

array directivity maximisation. Each scenario is run for ten trials and the best results are shown in Fig. 3. In case of full array, where no sub-arrays were implemented, best null depth achieved was −92 dB with array directivity 22.1 dBi. In comparison to uniformly excited full-array directivity of 23.1 dBi, the sector null is achieved at the loss of ∼1 dB in directivity.

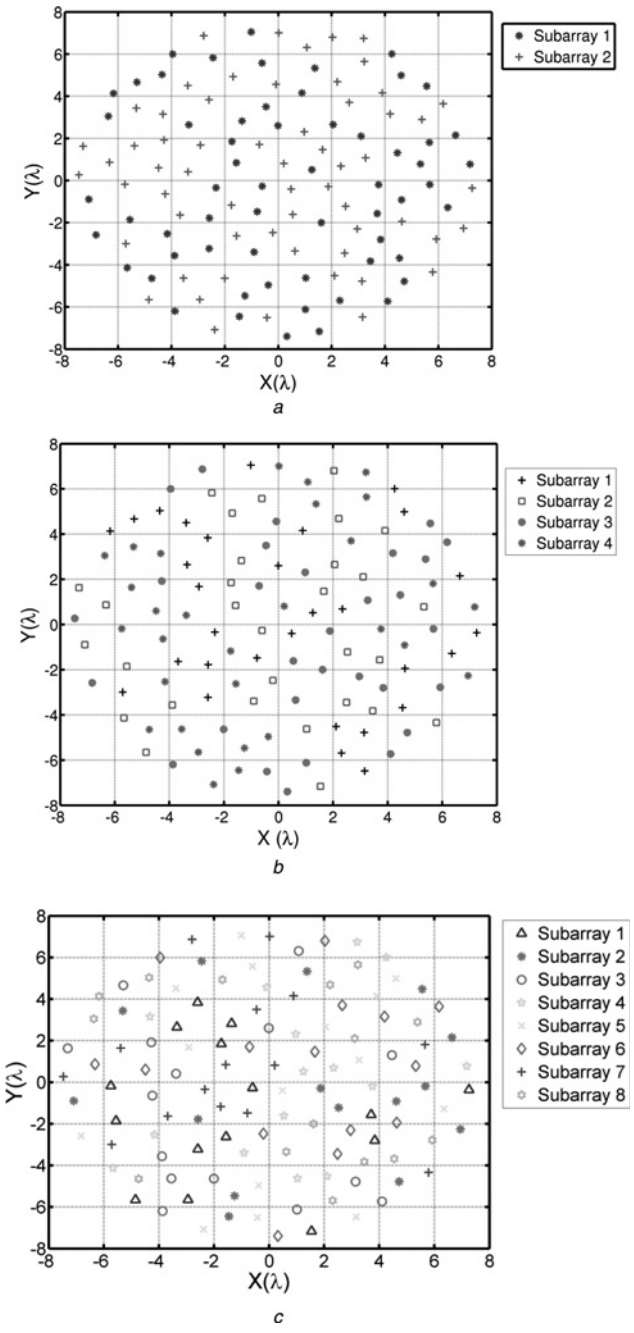

Fig. 2 *Element distribution in sub-arrays for N = 120*

a Config. #1, $M = 2$, $P = 60$
b Config. #2, $M = 4$, $P = 30$
c Config. #3, $M = 8$, $P = 15$

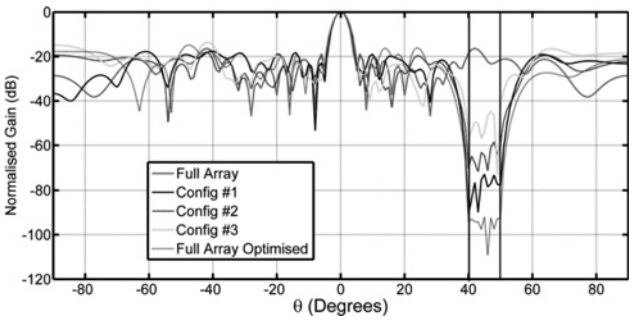

Fig. 3 *Radiation pattern comparison in $\varphi = 30^o$ plane, nulling sector $40^o \leq \theta \leq 50^o$*

Config. #1 has two sub-arrays and each of these sub-arrays is optimised independently for the same objective function and the derived weights applied to (3) to obtain the full-array pattern. The best achieved null depth and array directivity are recorded as −78 dB and 21.9 dBi, respectively. By running these two sub-arrays in parallel, convergence may be achieved 69% faster than the full-array optimisation. However, this comes at a cost, compared with the full-array scenario; null depth of Conf. #1 is slightly poor with similar directivity value. Table 2 compares the relative convergence times required to achieve presented results in Fig. 3. In case of Config. #2, four sub-arrays are optimised independently and superposition is applied to get the final radiation pattern presented in Fig. 3. The recorded null depth and directivity are −58 dB and 21.8 dBi, respectively. Since these sub-arrays have less number of elements and wider average inter-element separation compared with Config. #1, less control is exhibited in terms of null depth. Convergence result comparison shows that Config. #2 is 89% faster than the full array and 64% faster than the Config. #1. The Config. #3 offers fastest convergence and shows improvement over the full array, Config. #1 and Config. #2 by 96, 87 and 64%, respectively. However, the achieved null depth is the worse at −43 dB of all cases considered, but may well be acceptable for many applications. It has observed that compared with full optimised array, null depth deteriorates from Config. #1 to #3 as 15, 37 and 53% whereas deterioration in directivity is <5%.

Effect of sector width on null depth in all configurations has been summarised in Fig. 4 as it expands from $\theta = 40^o$ in $\phi = 30^o$ plane. It is important to note that maintaining a deep sector null is challenging

Table 2 Relative average computational time comparison for 1D single sector null (the reported comparison is based on ten trials of a sample case)

Array configuration	Relative computation time
full array	1
Config. #1	0.31
Config. #2	0.11
Config. #3	0.04

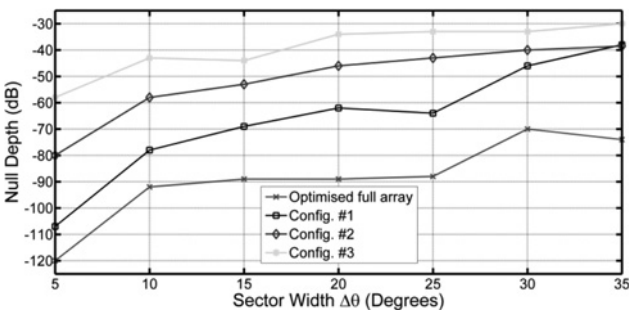

Fig. 4 *Comparison of sector width and null depth in $\phi = 30^o$ plane*

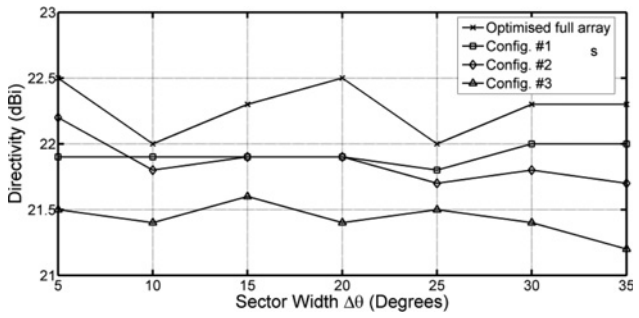

Fig. 5 *Comparison of sector width and array directivity in $\phi = 30^o$ plane*

with sub-arrays of fewer elements and wider element separation. Fig. 5 summarises the variation in directivity as it is evident that the use of aperture distributed sub-arrays has ensured similar HPBW and directivity in all configurations.

Fig. 6 presents radiation patterns in two ϕ principle planes and $\phi = 30^o$ plane for sector width $40^o \leq \theta \leq 65^o$. It can be seen that similar null depths were achieved due to the fact that sub-arrays consist of uniformly distributed elements.

Dual sector nulling is achieved by applying (6) in (4) and results are presented in Fig. 7. Target sectors were defined as $\Delta\theta_c' = -25^o \leq \theta \leq -20^o$ and $\Delta\theta_c'' = 50^o \leq \theta \leq 55^o$. The obtained null depths and directivity values are given in Table 3. With Config. # 1, combined dual band null depth was better than -60 dB and for Config. # 2 -45 dB.

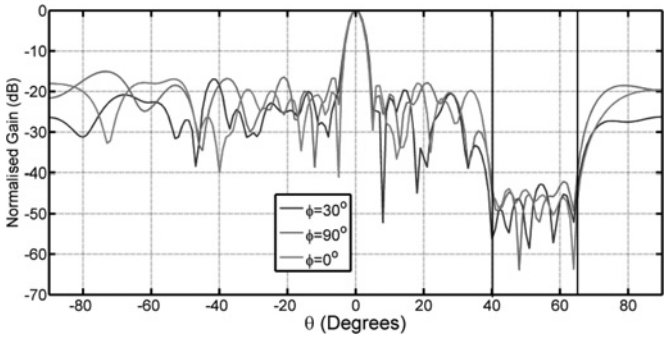

Fig. 6 *Radiation pattern obtained with Config. #2 in principle planes and $\phi = 30^o$ plane for imposed sector $40^o \leq \theta \leq 65^o$*

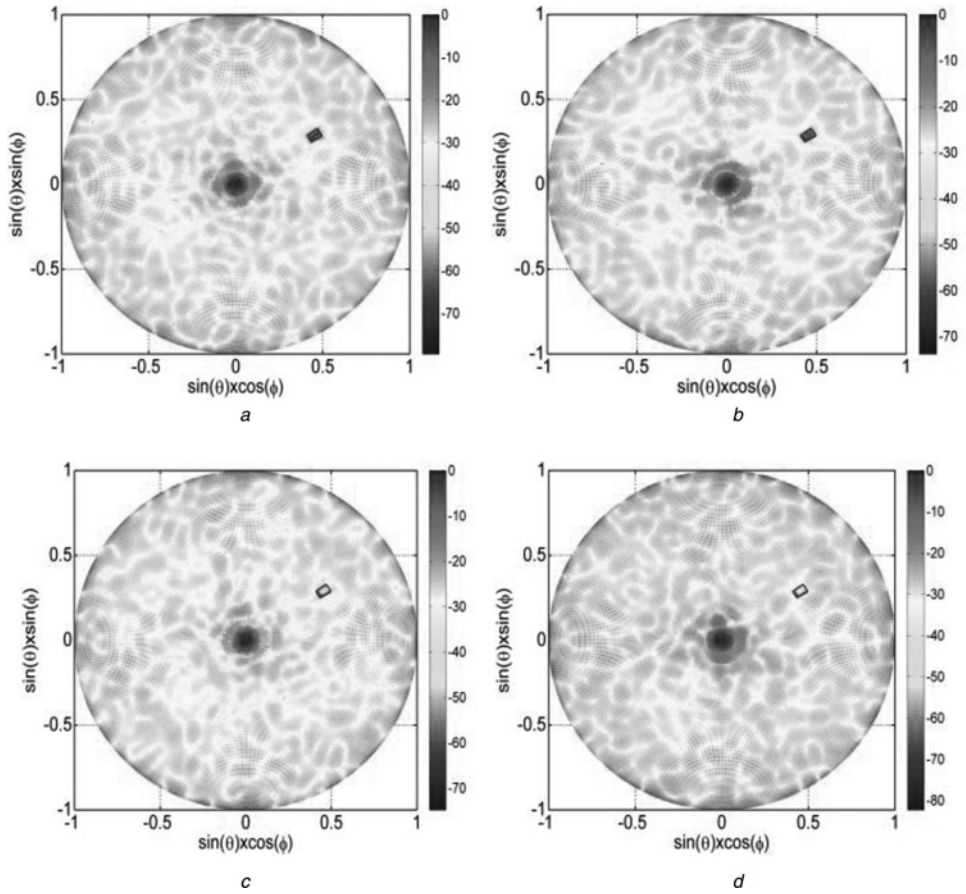

Fig. 7 *Best radiation patterns with 2D nulls out of ten trials for*

a Full array
b Config. #1
c Config. #2
d Config. #3 (rectangular outlines do not define the sector boundaries)

IET Microw. Antennas Propag., 2016, Vol. 10, Iss. 1, pp. 25–30

Table 3 Relative average computational time comparison for single sector 2D null (the reported comparison is based on ten trials)

Array configuration	Relative computation time
full array	1
Config. #1	0.38
Config. #2	0.16
Config. #3	0.05

Furthermore, the proposed scheme is demonstrated for achieving 2D nulls with sub-array configuration and performance is compared in terms of null depth and directivity. In Fig. 7*a*, best radiation obtained with full-array configuration is optimised to achieve a 2D null sector defined by $30^{o} \leq \theta \leq 35^{o}$ and $30^{o} \leq \phi \leq 35^{o}$. For full array, null depth obtained across the 2D sector was below −71.3 dB with array gain 22.5 dBi. Figs. 7*b–d* show patterns obtained with sub-array configurations. Best null depths out of ten trials for all three configurations from Config. #1 to #3 were found to be as low as −58.4, −41.1 and −30.4 dB with array gain maximised to 21.8, 21.7 and 21.6 dBi, respectively. The comparison of computational time has been given in Table 3.

The sub-arraying was also tested for the dual 2D sector nulling. In addition to the previously defined sector, an additional sector defined by $-60^{o} \leq \theta \leq -55^{o}$ and $30^{o} \leq \phi \leq 35^{o}$ was introduced. The best results obtained out of ten trials for each scenario have been shown in Fig. 8. Full-array scenario gives the null depth below −48.3 dB with 22 dBi array gain, and the radiation pattern is given in Fig. 8*a*. Radiation patterns of Config. #1 to #3 reported here in Figs. 8*b–d* are recorded to have null depths below −34.7, −29.2 and −26 dB with the array gain 21.6, 21.8 and 21.7 dBi, respectively.

On the comparison of Tables 2 and 3, it can be seen that similar relative convergence performances were achieved. However, it was observed that 2D sector nulls required approximately twice of the final convergence time compared with 1D sector null.

From the numerical examples presented in this work, it can be seen that the use of sub-arrays in sparse array antenna has successfully reduced the computational time with potential parallel processing. The obtained null depths and array gains with all sub-array configurations may be considered reasonable depending on the use of array antenna. The proposed aperture distributed sub-arrays may find its use in radars, radio astronomy and other sensing and imaging applications.

4 Conclusion

In this paper, it has shown that the sector nulling in large sparse array antennas may be achieved by implementing aperture distributed sub-arrays and performing sub-array optimisation in parallel. The technique is readily parallelisable and overhead time for each configuration can be normalised by finding the relative convergence time. The overall convergence time is defined by the latest convergence achieved by any sub-array. Therefore, the superposition process has to wait for the results from all sub-arrays to find the equivalent full-array radiation pattern. The sub-arrays with fewer elements will have fast convergence but due to large average element separation the null depth will compromise. The effect of the sector width on rejection performance has also been considered. It has found that wider sectors resulted in increased null depths. This situation worsens for the sub-arrays containing fewer elements. It has been shown that the proposed scheme may be used for other possible

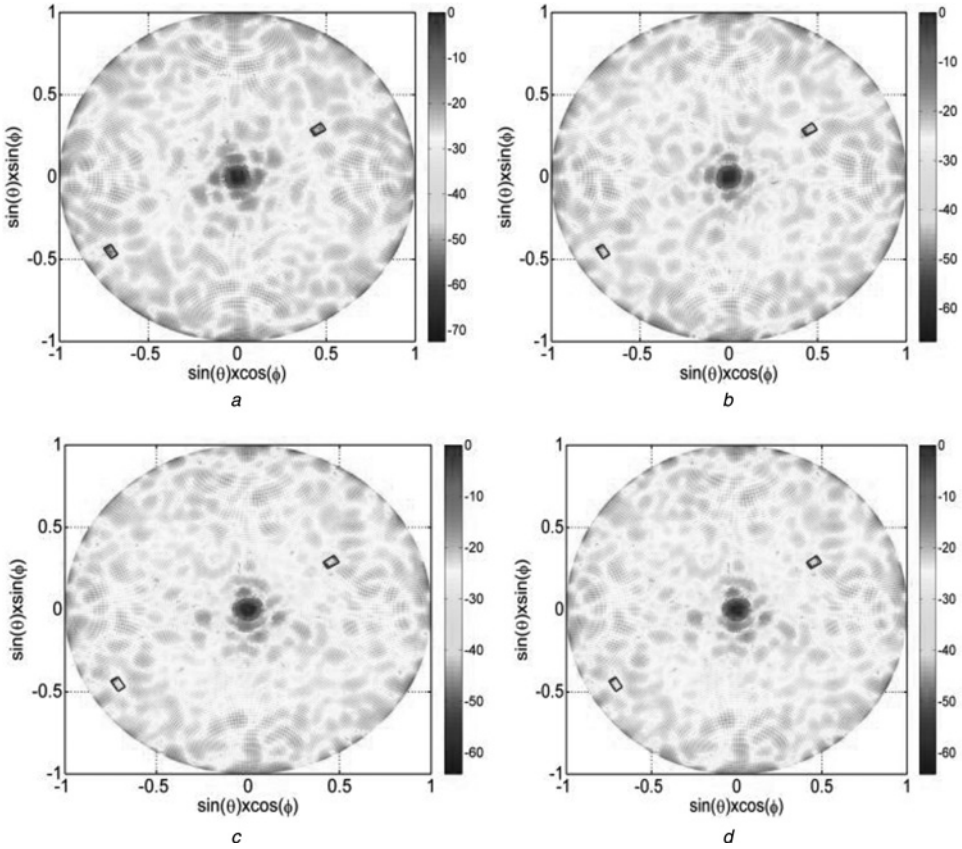

Fig. 8 *Best radiation patterns with dual 2D nulls out of ten trials for*

a Full array
b Config. #1
c Config. #2
d Config. #3 (rectangular outlines define the sector boundaries)

interference scenarios involving dual 1D, 2D and single sector 2D nulls.

It has been demonstrated that the proposed technique is useful for the optimisation of sparse arrays with average inter-element spacing greater than 1λ for sector nulling. The convergence time is significantly reduced by optimising the individual sub-arrays and applying superposition to find the full-array response. For the presented scenarios, the convergence achieved was up to 20 times faster with eight sub-arrays when compared with full-array optimisation.

5 References

1 Mailloux, R.J.: 'Array and sub-array pattern control features of sub-arraying feeds', *IEEE Trans. Antennas Propag.*, 1981, **29**, (3), pp. 538–544

2 Steyskal, H.: 'Wide-band nulling performance versus number of pattern constraints for an array antenna', *IEEE Trans. Antennas Propag.*, 1983, **31**, (1), pp. 159–163

3 Steyskal, H., Shore, R.A., Haupt, R.L.: 'Methods for null control and their effects on the radiation pattern', *IEEE Trans. Antennas Propag.*, 1986, **34**, (3), pp. 404–409

4 Meng-Hwa, E.: 'Linear antenna array pattern synthesis with prescribed broad nulls', *IEEE Trans. Antennas Propag.*, 1990, **38**, (9), pp. 1496–1498

5 Guella, T.P., Davis, R.M.: 'Synthesis of notched antenna patterns for wideband processing', *IEEE Trans. Antennas Propag.*, 1995, **43**, (12), pp. 1465–1471

6 Mismar, M.J., Ismail, T.H.: 'Partial control for wide-band interference suppression using eigen approach', *IEEE Trans. Antennas Propag.*, 1998, **46**, (4), pp. 600–602

7 Ismail, T.H., Dawoud, M.J.: 'Linear array pattern synthesis for wide band sector nulling', *Prog. Electromagn. Res.*, 1999, **21**, pp. 91–101

8 Mangoud, M.A., Elragal, H.M.: 'Wide null beamforming using enhanced particle swarm optimisation'. IEEE Ninth Malaysia Int. Conf. on Communications (MICC), 2009, pp. 159–162

9 Comisso, M., Vescovo, R.: 'Fast iterative method of power synthesis for antenna arrays', *IEEE Trans. Antennas Propag.*, 2009, **57**, (7), pp. 1952–1962

10 Corcoles, J., Gonzalez, M.A., Rubio, J.: 'Multiobjective optimisation of real and coupled antenna array excitations via primal-dual, interior point filter method from spherical mode expansions', *IEEE Trans. Antennas Propag.*, 2009, **57**, (1), pp. 110–121

11 Li, R., Xu, L., Shi, X.-W., *et al.*: 'Improved differential evolution strategy for antenna array pattern synthesis problems', *Prog. Electromagn. Res.*, 2011, **113**, pp. 429–441

12 Jianfeng, Y., Yufeng, W.: 'Synthesis of linear array with broad nulls using immune algorithm'. Ninth Int. Symp. on Antennas Propagation and EM Theory (ISAPE), 2010, pp. 1238–1241

13 Zheng, L., Shiwen, Y., Zaiping, N.: 'Pattern synthesis with specified broad nulls in time-modulated circular antenna arrays', *Electromagnetics*, 2011, **31**, (5), pp. 355–367

14 Keizer, W.P.M.N.: 'Amplitude-only low sidelobe synthesis for large thinned circular array antennas', *IEEE Trans. Antennas Propag.*, 2012, **60**, (2), pp. 1157–1161

15 Sayidmarie, K.H., Mohammed, J.R.: 'Performance of a wide angle and wide band nulling method for phased arrays', *Prog. Electromagn. Res.*, 2013, **33**, pp. 239–249

16 Mohammed, J.R., Sayidmarie, K.H.: 'Sidelobe cancellation for uniformly excited planar array antennas by controlling the side elements', *IEEE Antennas Wirel. Propag. Lett.*, 2014, **13**, pp. 987–990

17 Khan, A.A., Brown, A.K.: 'Null steering in irregularly spaced sparse antenna arrays using aperture distributed sub-arrays and hybrid optimiser', *IET Microw. Antennas Propag.*, 2014, **8**, (2), pp. 86–92

18 Kennedy, J., Eberhart, R.: 'Particle swarm optimisation'. Proc. of IEEE Int. Conf. on Neural Networks, 1995, vol. 4, pp. 1942–1948

19 Boggs, P.T., Tolle, J.W.: 'Sequential quadratic programming'. *Acta Numer.*, 1995, (4), pp. 1–51